Salty Matters

John Warren - Tuesday February 28, 2017

Evaporites and climate: Part 2 of 2 - Ancient evaporites and paleolatitudes

Introduction

Evaporites, along with coal and bauxites, are sediments considered to be climate sensitive. Ancient evaporite distribution and associated paleolatitudes are used to reconstruct the distribution of the world's arid belts across time. As we saw in Part 1 (Salty Matters, Tuesday, January 31, 2017), thick, widespread evaporite deposit are essentially a result of the atmospheric circulation of the Hadley cells. That is, locations of subtropical dry zones and tropical/subtropical deserts of the globe are mostly determined by the positions of subsiding branches of cool, dry descending air in a Hadley cells (aka Trade Wind Belt; Lu et al., 2007; Crowley and North, 1991) within low-lying regions tied a sufficient supply of mother brine. Thus, climate plus ongoing brine supply are the underlying factors controlling locales of significant evaporite deposition (Ziegler et al., 1981). The previous article focused on regional and local climatic controls across the Quaternary (Salty Matters, Tuesday, January 31, 2017). This article extends the time frame for the evaporite/climate association across the Phanerozoic and into the Precambrian.

As we move back in time, we move out of an ice-house-dominated world climate, with permanent ice caps waxing and waning at the world's poles, into greenhouse-dominant world climates. In greenhouse times there are no permanent polar ice sheet and glaciers occurred only in some high-altitude mountainous belts (Figure 1a, b). The transition into greenhouse climate changes the dominant 4th-order eustatic style from 100m amplitude changes every 100,000 years or so into 4th-order responses with much lower 3-5 m amplitude oscillations every 100,000 years (Figure 2a, b). Lack of polar caps raises world sealevel on the order of 40-50 metres. Thus, even without tectonic considerations, there is less continental freeboard in greenhouse times and increased the potential for significant cratonic coverage by epi-

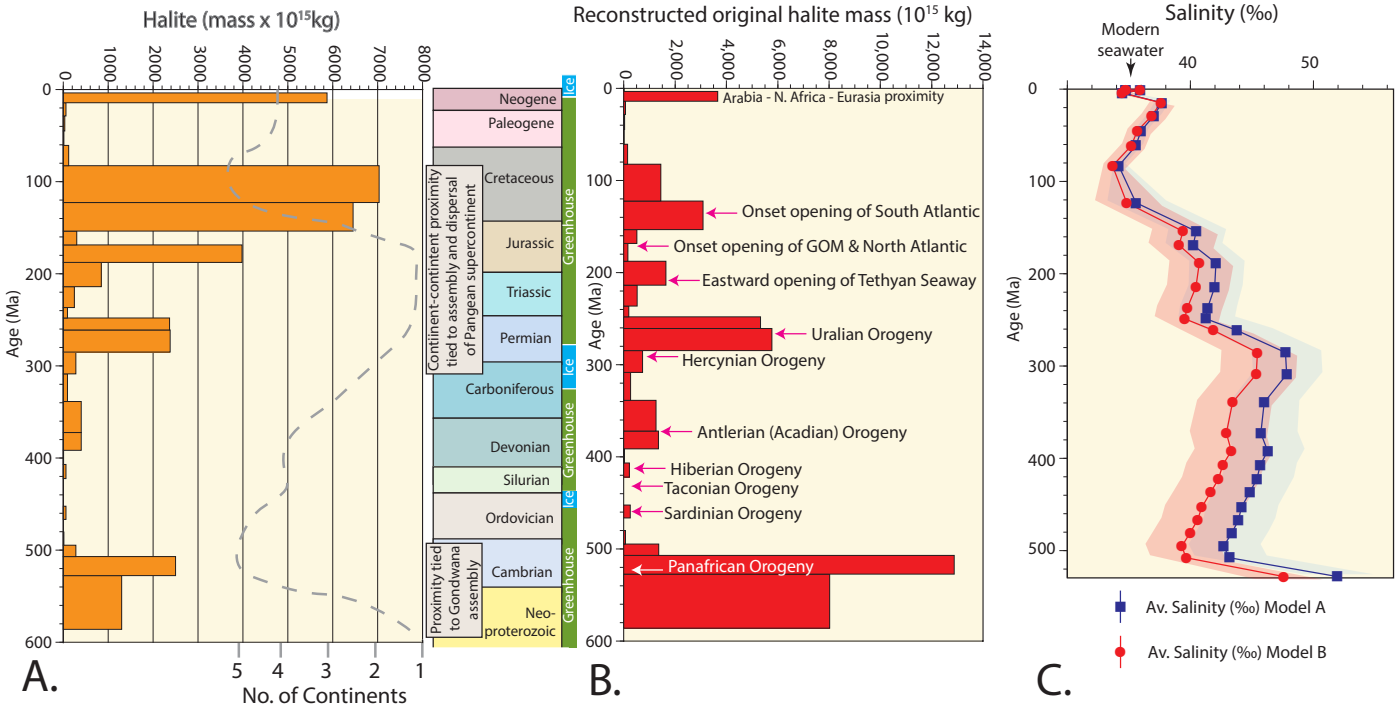

Figure 1. Phanerozoic evaporites in Deep Time (after Warren, 2010, 2016). A) Mass of Phanerozoic halite currently residing in the evaporite basin (after Hay et al., 2006; Number of continents curve from Condie 2004). B) Reconstructed mass of recycled Phanerozoic halite lost by combination of erosion and dissolution (after Hay et al., 2006). Time of halite precipitation as influenced by accretion and disintegration (dispersal) of Pangean supercontinent as well as other orogenic and tectonic events as shown (greenhouse after Fischer, 1981; tectonics after Haq and Van Eysinga, 1998; Haq and Al-Qahtani, 2005). C) Oceanic salinity changes for the last 500 my (after Hay et al., 2006).

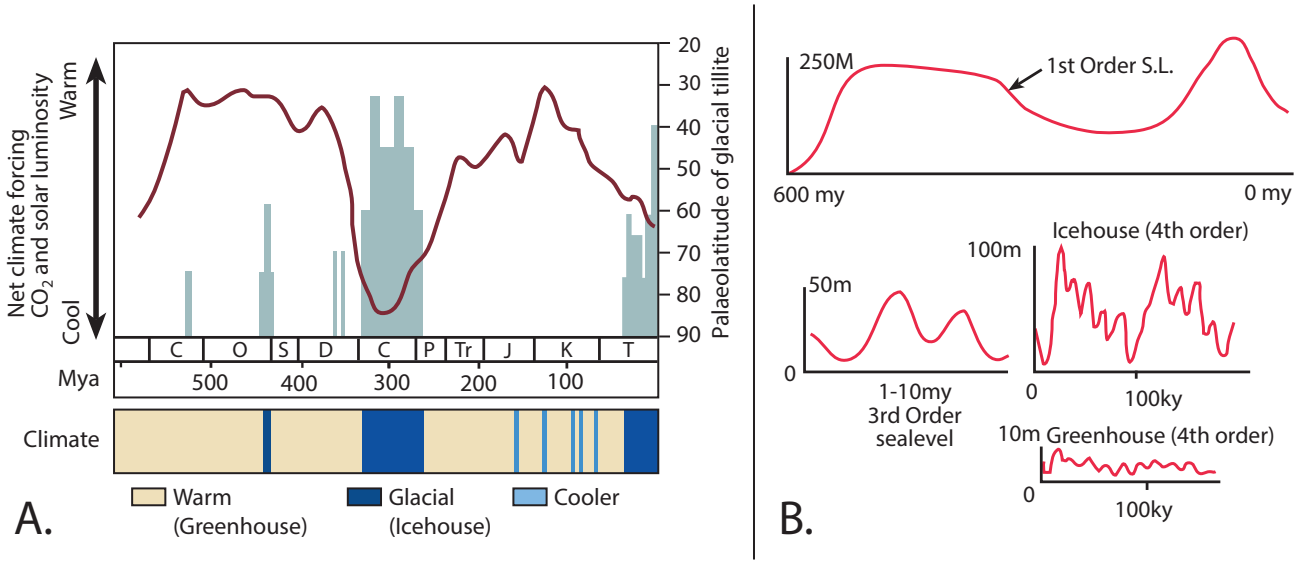

Figure 2. Relationship between icehouse and greenhouse conditions, eustasy and global CO2 (after Warren, 2016). A) Palaeolatitudinal extent of glacial tillite in relation to net forcing of climate due to variations in CO2 and solar luminosity. Inferred times of general greenhouse, icehouse and short cooler climate periods in Mesozoic (after Royer et al., 2004) B) Eustatic sealevel curves, showing first order Vail sealevel curve in the upper part. Rest of diagram plots typical amplitudes and periodicities of higher order sealevel curves. Third order curves have a 1-10 my periodicity. Schematic 4th order with superimposed 5th order sealevel curves are drawn for icehouse and greenhouse conditions (see text for explanation).

continental and pericontinental seaways (Warren, 2016; Chapter 5).

Looking back in time, beyond the last few million years of the Quaternary, means our conceptual models must encompass a broader range of tectonic settings as well as changes in the rates of seafloor spreading, supercontinents, and times of significant igneous outpourings (superplumes). All these additional world-scale variables across a longer set of available time explain the greater range of climate potentials on the earth, compared to anything that has occurred in the time-limited base seen in icehouse-dominant Quaternary climate spreads. The last few million years of the current icehouse mode is inhabited by the human species or its primate ancestors. The previous Icehouse dominant mode was in the Carboniferous-Mid Permian when the dominant land animals were amphibians and primitive reptiles.

One the first questions this broader ancient climate spectrum, tied to evaporites over deep time, offers up is; "How do the positions of Hadley cells vary across geological time frames?" In part 1, we saw how the rise of the Himalayas deflected a belt of cool, dry descending air much further south toward the Equator. Moving back in time creates a broader scaffolding for documenting climate variation, in part driven by the rise and fall of mountain ranges, but also influenced by increases in the rate of seafloor spreading driving ocean basin shallowing and by changes in atmospheric/seawater compositions and temperatures.

Hadley cells and latitudinal variability over time

According to Chen Xu et al., 2013 and Boucot et al., 2013, much of the world-scale Phanerozoic distribution of significant bedded evaporite accumulations indicates the ongoing presence of two mid-latitude arid belts, presumably situated beneath Hadley Cells. There are exceptions in locales generated in local rain shadows with orographic control provided by neighbouring mountain ranges. However, in the later Permian, through the Triassic, and much of the Jurassic the two formerly mid-latitude Hadley Cells merged over the more central Pangaeanic regions of Africa, Europe and the adjacent Americas, to form an arid belt that also encompassed low-latitude, equatorial arid regions (Figure 3). Across the continental interior of the Pangean supercontinent, this arid to hyperarid equatorial belt in the supercontinent interior prevented the formation of climate-sensitive sediments that are more typical of humid equatorial conditions that deposit coals, kaolinites, lateritic materials and bauxites. However, in this same time interval, these more humid sediment products are typically present at low latitudes of these time slices adjacent to the Panthalassic ocean.

That is, in the absence of an equator-spanning supercontinent, low latitudes, typically imply humid and non-seasonal tropical conditions throughout much of the Phanerozoic, as we see today. But the assembly of the Pangaean supercontinent disrupted this latitudinally-zoned atmospheric circulation, replacing it with a progressively more monsoonal (seasonal) circulation and

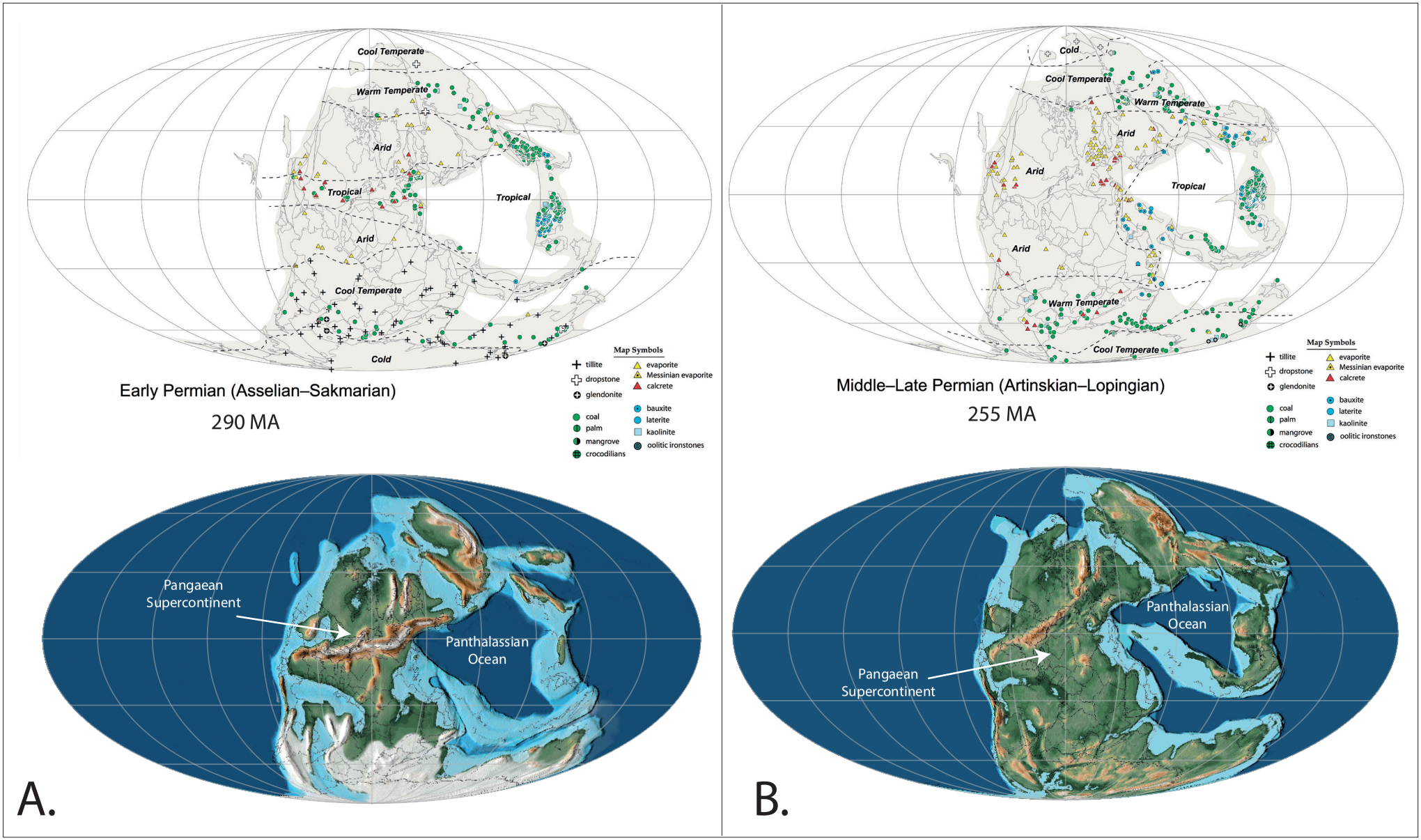

Figure 3. Permian palaeoclimatic reconstructions of the Pangaean Supercontinent redrafted and replotted from Boucot et al. 2013, and the Scotese PaleoAtlas mounted in GPlates 2.0. A) Reconstruction of Pangaea, some 290 Ma, with ice sheets at the southern Pole and a well-developed tropical corridor indicated by climate-sensitive deposits. B) Reconstruction of Mega-monsoonal Pangaea, some 255 Ma, showing the lack of tropical sediment indicators outside the region surrounding the Panthalssian ocean.

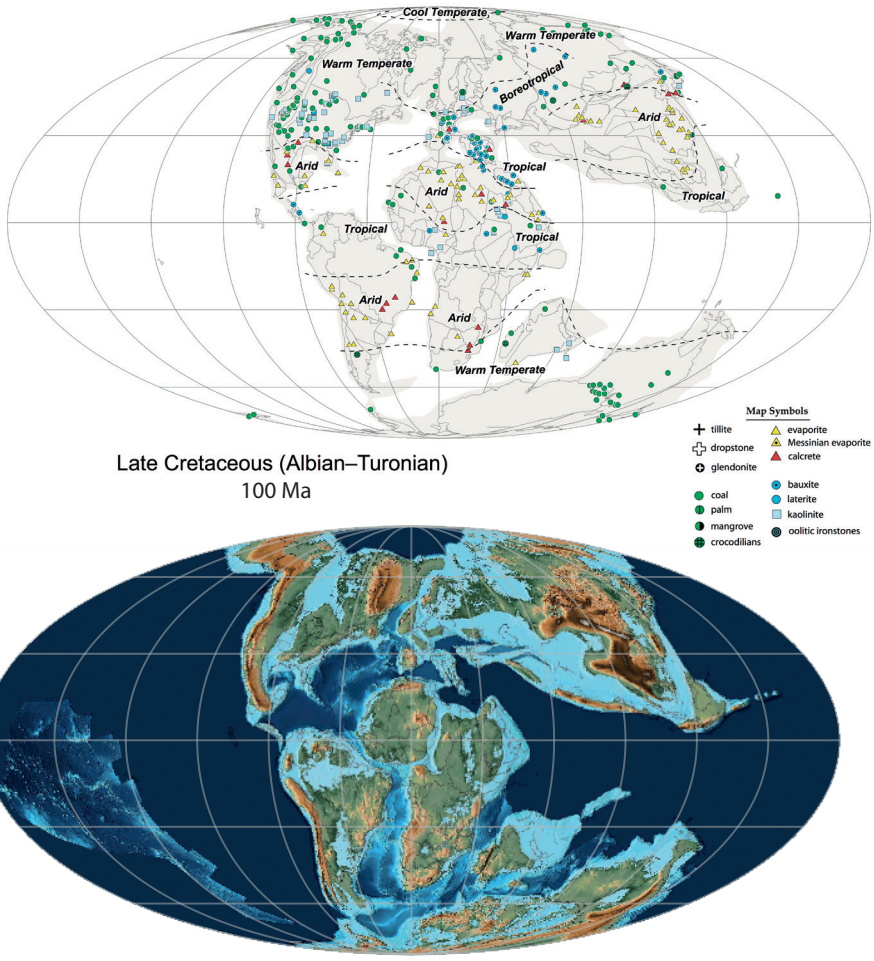

Figure 4. Late Cretaceous (100 Ma) palaeoclimatic reconstructions post-breakup of the Pangaean Supercontinent redrafted and replotted from Boucot et al. 2013, and the Scotese PaleoAtlas mounted in GPlates 2.0. Shows a tropical equatorial corridor has developed once more, as indicated by climate-sensitive deposits.

more arid, at times hyperarid, conditions in the equatorial continental interior of Pangaea (Parrish, 1993). The Pangean supercontinent reached its maximum areal extent in the Triassic and was associated with what is known as the Pangaean Megamonsoon. There were immense arid regions across the interior regions of the supercontinent that were nearly uninhabitable, with scorching days and frigid nights. However, Panthalassian coasts still experienced seasonality, transitioning from rainy weather in the summer to dry conditions during the winter and the associated accumulation of humid sediments (Figure 3b; Boucot et al., 2013). Megamonsoon aridity is evidenced not just in the accumulation of low-latitude bedded evaporite deposits. Low latitude continental aridity also drove the accumulation of thick, widespread low-latitude desert redbeds, sourced by eolian, not fluvial, detrital transport (Sweet at al., 2013) and the precipitation of bedded salt crusts in ephemeral saline lakes under exceptionally-high surface temperatures of up to 73°C (Zambito and Benison, 2013).

Paleolatitude reconstructions Chen-Xu et al. (2013) show these continental interior arid belts in low latitude tropical-subtropical regions persisted from the Permian to the Early Cretaceous. Reunion of the humid regions from both sides of Pangaea by the early Late Cretaceous formed a through-going low latitude humid tropical-subtropical belt. This coincides with the disaggregation of Pangaean supercontinent, as the initial stages of a modern latitudinal climate belt distribution pattern emerged, tied to latitudinally-restricted evaporites that continue to the present (Figure 4).

Tectonism and eustacy in arid climates drive the formation of mega-evaporite basins

Within this Phanerozoic climatic framework, there are times when significant volumes of evaporites form what are know as saline giants, or megahalite/megasulphates deposits. These massive accumulations of salts formed beneath arid climates that can span both greenhouse and icehouse climates (Figure 1; Warren, 2010, 2016). Ancient marine saline giants (megahalites and megasulphates) accrued in either of two plate-scale settings, which at times merged into one another, namely; 1) Platform evaporites (Figure 5) and, 2) Basinwide evaporites (Figure 6).

The first major contrast with nonmarine continental dominance in Quaternary evaporite settings is the fact that platform evaporites require greenhouse eustasy a and a marine feed, the second is that basinwide evaporites require tectonically- and hydrographically-isolated widespread subsealevel depressions, typically found along plate edges with continent-continent proximity in regions with a marine seepage feed and/or periodic marine overflows (Figure 6). Neither platform or basinwide conditions are present on the current earth surface. For basinwides, suitable hydrologic conditions were last present during the Messinian Salinity Crisis in the Mediterranean region, and platform evaporite settings were last present on earth across large parts of the Middle East carbonate platform during the Eocene (Tables 1, 2). There is a third group of ancient evaporite deposits; it encompasses all

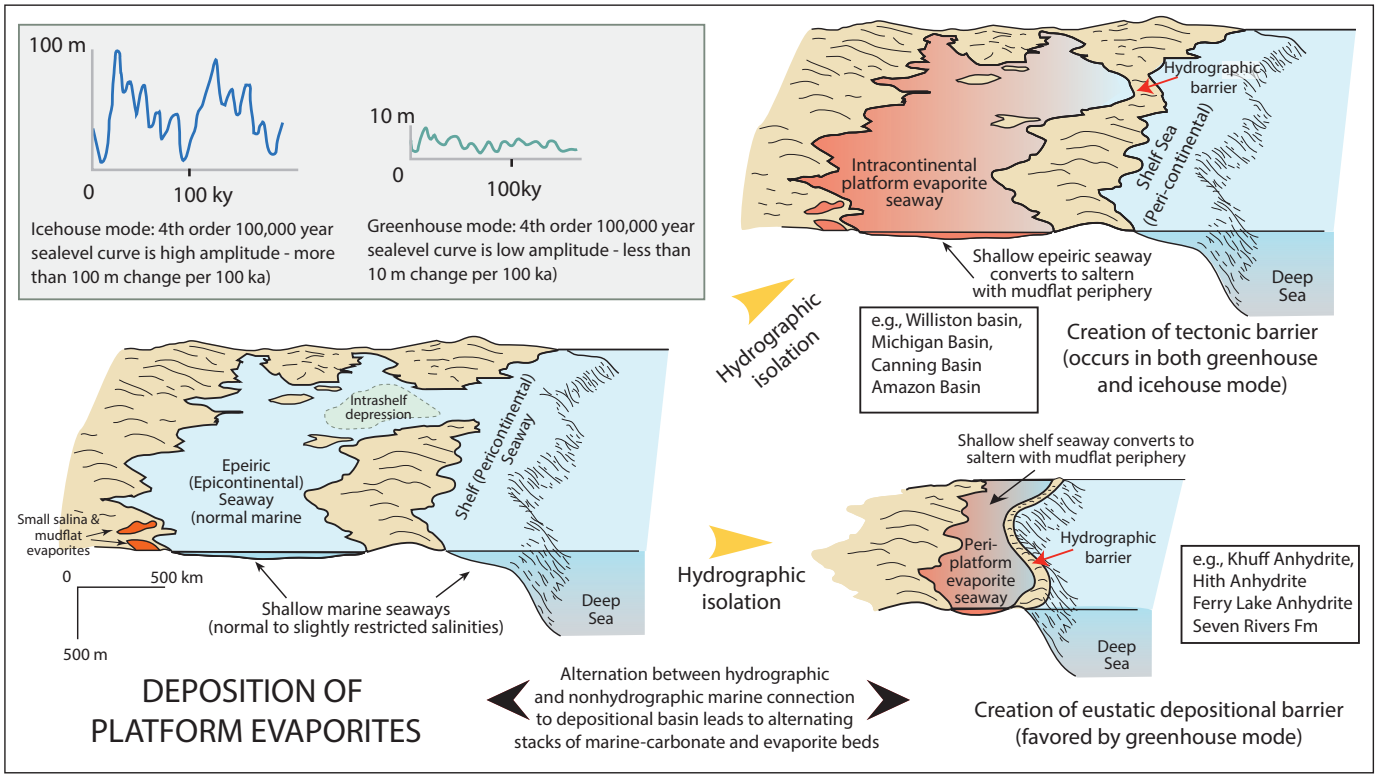

Figure 5. Epeiric (epicontinental) seaways that covered large areas of the continental interior with shallow marine waters are known as intracratonic basins, while epeiric seaways that formed as very wide shelf edges along the continental margin as known as pericontinental seaways. Waters were very shallow over areas that were hundreds to thousands of kilometres across. Neither setting has a modern counterpart; pericontinental seaways that evolve into salterns and or evaporitic mudflats are more typical of marine-margin eustatic styles on the earth in greenhouse climate mode, when the lack of permanent polar icecaps, especially coupled with higher rates of seafloor spreading, meant the continental freeboard was much larger than it is today (after Warren, 2010, 2016).

nonmarine lacustrine beds past and present (Table 3). This group has same-scale modern-ancient counterparts, unlike ancient marine platform and basinwide evaporites (Warren, 2010, 2016). Interestingly, the lacustrine depositional style for bedded salt accumulation dominates in the icehouse climate that is the Quaternary, and so biases a strictly uniformitarian view of the past with respect to the relative proportions of nonmarine versus marine evaporite volumes (see Part 1; Salty Matters, Tuesday, January 31, 2017).

Platform evaporites

Are made up of stratiform beds, usually <50 m thick and composed of stacked <1 to 5 m thick parasequences or evaporite cycles, with a variably-present restricted-marine carbonate unit at a cycle base (Table 1). Salts were deposited as mixed evaporitic mudflat and saltern evaporites, sometimes with local accumulations of bittern salts. Typically, platform salts were deposited in laterally extensive (>50-100 km wide), hydrographically-isolated, subsealevel marine-seepage lagoons (salterns) or evaporitic mudflats (sabkhas and salinas). These regions have no same-scale modern counterparts and extended as widespread depositional sheets across large portions of hydrographically isolated marine platform areas that passed seaward across a subaerial seepage barrier into open marine sediments (Figure 5). In marine margin epeiric settings, such as the Jurassic Arab/Hith and Permian Khuff cycles of the Middle East or the Cretaceous Ferry Lake Anhydrite in the Gulf of Mexico, these platform evaporites are intercalated with shoalwater marine-influenced carbonate shelf/ramp sediments, which in turn pass basinward across a subaerial sill into open marine carbonates. Landward they pass into arid zone continental siliciclastics or carbonate mudflats.

Platform evaporite deposition occurred in both pericontinentaand epicontinental settings, at times of low-amplitude 4th and 5th order sealevel changes, which typify greenhouse eustasy (Figure 5; Warren, 2010). Platform evaporites also typify the saline stages of some intracratonic basins. Platform evaporites cannot form in the high-amplitude, high-frequency sealevel changes of Icehouse eustasy. The 100m+ amplitude oscillations of Icehouse times mean sealevel falls off the shelf edge every 100,000 years, so any evaporite that had formed on the platform is subaerially exposed and leached. Fourth order high-amplitude icehouse eustatic cycles also tend to prevent laterally-continuous carbonate sediment barriers forming at the top of the shelf to slope break, and so icehouse evaporite systems tend not to be hydro-graphically isolated (drawdown) at the platform scale. Rather icehouse eustasy favours nonmarine evaporites as the dominant style, along with small ephemeral marine-margin salt bodies, as seen today in the bedded Holocene halites and gypsums of Lake Macleod in coastal West Aus-

Platform successions	Age	Comments
Rus Fm., Arabian Basin, Qatar, Saudi Arabia	Eocene, Lower	Has a total thickness of about 100 m, composed of limestones and dolomitic limestones (often argillaceous) passing upward into massive 10m thick saltern anhydrite
Ferry Lake Anhydrite, NE Gulf coast, USA	Cretaceous, Lower	Divided in 9 individual saltern anhydrites that are traceable from southern Mississippi to southern Florida and intercalated with normal marine bioclastic limestones
Smackover/Buckner Fm., N Gulf Coast, USA	Cretaceous, Lower	Buckner Anhydrite made up of intercalated 2-6m thick saltern anhydrites and marine limestones. It extends from Florida Panhandle to South Texas
Hith Anhydrite, Arabian Basin, Middle East	Jurassic, Upper	Hith anhydrite is a regional seal that extends across much of the Arabian Peninsula and locally reaches 170 m in thickness. It is composed of bluish-gray to alternating bands of blue and white anhydrite with two internal carbonates and separates marine carbonates of underlying Arab Fm from overlying Yamama (unconformable base).
Middle Anhydrite Marker, Khuff Fm., Middle East	Permian, Upper	Middle Anhydrite can be traced from eastern Saudi Arabia to offshore UAE, and reaches the onshore Fars Province of Iran. This anhydrite is some 12–17 m (20–39 ft) thick and consists of massive saltern anhydrite with minor thin interbeds of dolomite
San Andres Fm., Northern Delaware Basin margin, USA	Permian, Upper	Anhydrite occurs as widespread saltern units composed of massive nodular mosaic anhydrite beds up to 5m thick capping cyclic shoaling variably-dolomitised platform carbonates. Individual anhydrite beds (P1-P5) that can be traced from Palo Duro basin into shelf edge of the Slaughter-Levelland trend
Cadjebut Fm., Canning Basin margin, Australia	Devonian, Middle	Saltern anhydrites up to 5m thick extend across a Devonian platform embayment pass and pass laterally into the sulphide mineralised ore horizons of the Cadjebut Mine region. Saltern sulphates capped shoaling oncolitic and bioclastic muds that overlie normal marine grainstones and wackestones
Cool Creek Fm., Arbuckle platform, USA	Ordovician, Lower	At least three 1-2 m thick breccias, interpreted to be of solution collapse origin, are present in the Cool Creek and define the presence of former widespread saltern anhydrite units that capped restricted marine stromatolitic carbonate platform sediments
Red Heart Dolomite, Georgina Basin, Australia	Cambrian, Lower-Middle	Red Heart Dolomite which extends across much of Central Australia is a completely dolomitised 100m-thick platform carbonate deposited in an evaporitic shallow-water epeiric seaway It is characterized by at least four shallowing-upwards saltern anhydrite-capped cycles. Many of the surface and near-surface anhydrites caps are now leached and represented by collapse breccias
Intracratonic platform evaporite successions	Neoproterozoic to Eocene	North Sahara Basin, Africa; Canning Basin, Australia; Muschelkalk and Paris Basins, SW Germany and Spain; Amazonas Basin, South America; West Siberian Basin, Russia; Michigan Basin and Williston Basin, USA (see Table 2)

Table 1. Selected platform evaporite examples (see Warren 2016; Chapter 5 for deposit details and listing of relevant citations)

tralia (Part 1; Salty Matters, Tuesday, January 31, 2017).

Ancient platform evaporite successions may contain halite beds, especially in intracratonic basinwide settings, but periplatform settings, outside of intracratonic basins, are typically dominated by 5–40 m thick Ca-sulphate beds intercalated with normal-marine platform carbonates (Table 1). The lateral extent of these epeiric platform sulphate bodies, like the Middle Anhydrite Member of the Permian Khuff Fm. of Saudi Arabia and the UAE, with a current area of more than 1,206,700 sq. km., constitute some of the most aerially-extensive evaporite beds ever deposited.

Basinwide evaporites

Are made up of thick evaporite units >50–100 m thick made up of varying combinations of deepwater and shallow water evaporites (Figure 1; Table 2). They retain textural evidence of different but synchronous local depositional settings, including mudflat, saltern, slope and basin (Figure 6). When basinwide evaporite deposition occurs, the whole basin hydrology is evaporitic, holomictic, and typically saturated with the same mineral phase across vast areas of the basin floor, as seen on a much smaller scale today in the Dead Sea basin. The Dead Sea currently has halite forming simultaneously as; 1) decimeter-thick chevron-dominated beds on the saline-pan floor of the shallow parts around the basin edge in waters typically less than 1-10 metres deep, and 2) as coarse inclusion-poor crystal meshworks of halite on the deep basin floor that sits below a halite-saturated brine column up to hundreds of metres deep. Ancient basinwide successions are usually dominated by thick massive salt beds, generally more than 100-500 m thick. Deposits are made up of stacked thick halite beds, but can also contain substantial volumes of thick-bedded Ca-sulphate and evaporitic carbonate, as in the intracratonic basinwide accumulations of the Delaware and Otto Fiord Ba-sins (Table 2).

Owing to inherent purity and thickness of the deposited halite, many halite-dominant basinwide beds are also remobilized, via loading or tectonics, into various halokinetic geometries (Hudec and Jackson, 2007). Some basinwide systems (mostly marine-fed intracratonic settings) entrain significant accumulations of marine-fed potash salts, as in the Devonian Prairie Evaporite of western Canada. In contrast, all Quaternary examples of commercial potash deposits are accumulating in continental lacustrine systems (Warren 2016; Chapter 11).

Basinwide evaporite deposits are the result of a combination of tectonic and hydrological circumstances that are not currently active on the world's surface (Figure 1). They were last active in the Late Miocene (Messinian), in association with soft-suture collision basins tied to the Alpine-Himalaya orogenic belt, and in Middle Miocene (Badenian) basins developed in the early rift stages of the

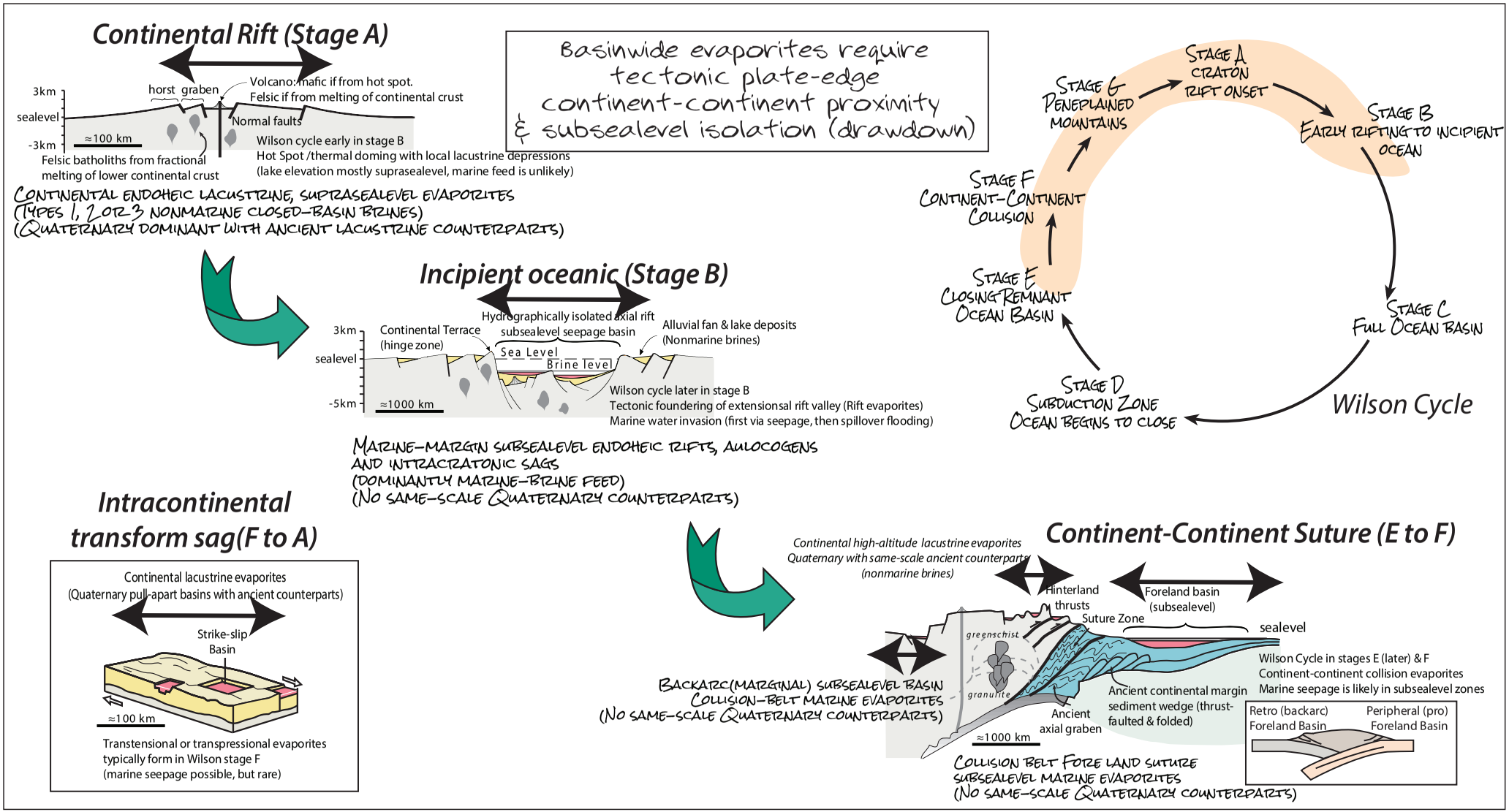

Figure 6. Tectonic and hydrographically isolated (marine endorheic) continent-margin situations where basinwide evaporites tend to accumulate (evaporite beds are shaded pink). Positions are largely tied to world-scale times of continent-continent proximity and so can be tied to the various stages of the Wilson Cycle, so basinwides are tied to tectonics and can span greenhouse and icehouse climate modes(After Warren, 2010, 2016).

Sequence of interest	*Basin/setting and Location*	*Age*	*Basin style*	*Tectonic event*
Messinian Evaporites	Lago-Mare ("lake sea"), Mediterranean	Miocene, Upper	Flexure	Convergent foreland, Alpine orogeny
Belayim and Gharib formations	Gulf of Suez - Red Sea, Middle East	Miocene, Middle - Upper	Extension	Red Sea Breakup and the formation of the Red Sea/ Suez Rift
Gachsaran Formation	Mesopotamian Basin, Middle East	Miocene, Middle	Flexure	Convergent foreland Zagros-Taurus
Maha Sarakham Formation	Khorat Basin, Thailand	Cretaceous, Upper	Flexure	Convergent foreland Cretaceous inversion and thrust loading
Todilto Formation	Todilto Basin, New Mexico, USA	Jurassic, Middle	Flexure	Convergent foreland Ancestral Rockies
Louann Salt	Gulf of Mexico Basin, Gulf Coast	Jurassic, Middle	Extension	Incipient Gulf of Mexico- Atlantic rift
Argo Formation & Osprey Evaporites	Scotian Basin, and Grand Banks, Canada	Upper Triassic-Lower Jurassic	Extension	Incipient Atlantic rifting
Northwich Halite	Cheshire Basin, United Kingdom	Triassic	Extension	Incipient Atlantic rifting
Halite (S1-S4, Las and Dogger Anhydrite units)	Oued Mya Basin, Algeria, Northern Sahara	Upper Triassic-Lower Jurassic (Liassic)	Extension	Intraplate sag basin atop grabens created by incipient Atlantic and Tethyan rifting
Saliferous units	Ghadames (Berkine) Basin, Algeria	Triassic, Upper Jurassic, Lower	Extension	Intraplate sag basin atop grabens created by incipient Atlantic and Tethyan rifting
Argiles d'Argana	Essaouria Basin, Morocco	Triassic, Upper	Flexure	Intraplate sag basin atop grabens created by incipient Atlantic and Tethyan rifting
Formation Salifere	Saharan Atlas, Algeria	Triassic, Upper	Flexure	Intraplate sag basin; incipient Atlantic and Tethyan rifting
Salina d'Ourgla	Northern Sahara Salt Basin, Algeria	Triassic, Upper	Flexure	Intraplate sag basin; incipient Atlantic and Tethyan rifting
Nikitov, Slavyan, and Kramatov Formations	Dnieper-Donets Basin, Ukraine and Russia	Permian, Lower (Kungurian salt)	Flexure	Post-rift sag reactivated by Uralian Orogeny (Hercynian)
Rotliegende Group	Dniepr-Donets Basin, Eastern Europe	Permian, Lower	Flexure	Foreland Variscan Orogeny
Zechstein Basin, NW Europe	NW European Basin, NW Europe	Permian, Upper	Flexure	Post Variscan Orogeny collapse
Castile Formation	Delaware Basin, West Texas	Permian, Upper	Flexure	Marathon-Ouchita
Iren Horizon Kungurian evaporites	North Caspian Basin (aka Pri- or Peri-Caspian), Khazakhstan and Russia	Permian, Lower	Flexure	Foreland, Uralian Orogeny. Collision of Russian Platform with the Siberia/Kazakhstan block
Otto Fiord Formation	Sverdrup Basin, Canadian Arctic Islands	Carboniferous	Extension	Synrift stage of post-Caledonian intracontinental rifting
Paradox Formation	Paradox Basin, Colorado-Utah USA	Carboniferous, Upper	Flexure	Ancestral Rockies
Caurauri Formation	Amazonas Basin, South America	Carboniferous, Upper	Flexure	Distal effect of Marathon-Ouchita orogeny
Windsor Group	Magdalen Basin, Eastern Canada	Carboniferous, Lower	Extension	Cabot fault-Belle Isle transtensional system
Liven Horizon	Dniepr-donets Basin, Ukraine and Russia	Devonian, Upper Frasnian and Famennian	Extension	Synrift via crustal stretching (passive margin)
Prairie Evaporite	Elk Point Basin, Western Canada Plains	Devonian, Middle	Flexure	Intracratonic sag; a distal effect of thrust-loaded compression of the western Laurasian plate
Salina Group	Michigan Basin, USA	Silurian, Middle-Upper	Flexure	Intracratonic sag during Taconian thrust loading, sits atop Mesoproterozoic Midcontinent rift basin
Mallowa Salt (Carribuddy Formation)	Canning Basin, Northwest Australia	Ord. -Silurian	Extension	Pre-rift to Synrift stage of intracratonic sag
Chandler Formation	Amadeus Basin, Central Australia	Cambrian, Lower	Flexure	Petermann Range Orogeny - Gondwana Accretion
Lower and upper Usolye Group	Turukhan - Irkutsk - Olekmin salt basin, SE Siberian Craton	Late Neoproterozoic (Vendian)-early Cambrian	Flexure	Intracratonic Sag- Gondwana assembly
Hormuz Formation	Arabian Basin, Middle East	Late Neoproterozoic- early Cambrian (550 Ma)	Compression	Collision flexure - Pan African Orogeny; Gondwana Accretion
Ara Salt, Oman	Fahud, Gaba and South Oman Salt Basins, Oman	Late Neoproterozoic- early Cambrian (550 Ma)	Compression	Collision flexure - Pan African Orogeny; Gondwana Accretion
Bitter Springs Formation	Amadeus Basin, Central Australia	Early Neoproterozoic (≈ 800 Ma)	Extension- intracratonic sag	Rift - Rodinia breakup
Callana Formation	Adelaide Geosyncline, South Australia	Early Neoproterozoic (≈ 800 Ma)	Extension- intracratonic sag	Rift - Rodinia breakup
Browne Fm	Officer Basin, West Australia	Early Neoproterozoic (≈ 800 Ma)	Extension- intracratonic sag	Rift - Rodinia breakup

Table 2. Selected basinwide evaporite examples classified by age and tectonic setting (see Warren 2016; Chapter 5 for deposit details and listing of relevant citations)

Red Sea. Basinwide systems will be active again in the future at sites and times of appropriate plate-plate interaction, when two continental plate edges are nearby, and the intervening seafloor is in or near a plate-edge rift or suture and is both subsealevel and hydrographically isolated (Figure 6). Unlike most platform evaporites, basinwides do not require greenhouse eustacy, only the appropriate association of arid climate and tectonics. The latter sets up a deep hydrographically-isolated subsealevel tectonic depression with a geohydrology that can draw on a huge reserve of marine mother brine in the nearby ocean. For this reason, saline giants tend to form at times of plate-scale continent-continent proximity and so occur mostly in craton-margin settings.

Lacustrine (nonmarine) evaporites

Quaternary continental playa/lacustrine are constructed of stratiform salt units, with the greater volume of saline sediment accumulating in lower, more-saline portions of the lacustrine landscape. Beds are usually dominated by nodular gypsum and displacive halite, deposited in extensive evaporitic mudflats and saltpans with textures heavily overprinted by capillary wicking, rather than as bedded bottom-nucleated layers on the subaqueous floors of perennial brine lakes (Ruch et al., 2012). In ancient counterparts, the total saline lacustrine thickness ranged from meters to hundreds of meters, with lateral extents measured in tens to hundreds of kilometres (Table 3). Lacustrine salt beds are separated vertically, and usually surrounded by, deposits of lacustrine muds, alluvial fans, ephemeral streams, sheet floods, eolian sands, and redbeds. As today,

Sequence of interest	*Basin/setting*	*Locality*	*Age*
Beds of displacive borates	Bigadic, Emet and Kirka basins	Turkey	Neogene
Gypsiferous Blanchetown Formation	Palaeolake Bungunnia	Murray Basin, Australia	Neogene
Massive halite of Salar Grande	Cordillera de la Costa forearc	Central Andes, Chile	Neogene
Bed I and Bed II	Olduvai Gorge, East African Rift	Tanzania	Pliocene
Furnace Creek Fm. (borate beds)	Extensional half-graben	Death Valley, USA	Pliocene-Miocene
Gypsum as beds and fracture-fills	Sivrihisar/Sultancayir/ Cankiri basins	Anatolia, Turkey	Miocene
Lacustrine carbonates	Ries-impact-crater	Southern Germany	Miocene
Lacustrine halite, 2.5 km thick	Hualapai basin	NW Arizona	Miocene
Kirmir Fm.	Beypazari Basin	NW Turkey	Miocene, Middle - Upper
Juncalito Fm.	Puna Plateau - intra-arc basin	NW Argentina	Miocene, Middle -Upper
Bedded and nodular gypsum (glauberite)	Calatayud Basin	Spain	Miocene, Lower
Bedded and nodular gypsum (glauberite)	Ebro Basin - foreland basin	Spain	Miocene, Lower
Creede Fm.	Ancient Lake Creede	Colorado, USA	Oligocene, Upper
Potash beds of Couche Inferieure	Mulhouse Basin	Rhine Graben, Europe	Oligocene, Lower
Green River Fm.	Uinta and Piceance basins	Utah and Colorado	Eocene
Bembridge Limestone Fm.	Isle of Wight	Southern England	Eocene, Upper
Taleh Fm.	Somalia	El Bur Plateau	Eocene, Lower -Middle
La Tinaja del Oso (colemanite)	Magdalena extension basin	Mexico	Mid-Tertiary
Uhangri Fm.	Yucheon Group	SW Korea	Cretaceous
Mmashoro Fm.	Basal Kalahari Group	Botswana	Cretaceous, Upper
El Molino Fm.	Potosi Basin	Bolivia	Cretaceous, Upper - Tertiary, Lower
Lagoa Feia Fm.	Campos Basin	Brazil	Cretaceous, Lower
Codocedo Limestone Member	Atacama region	Northern Chile	Jurassic, Upper - Cretaceous, Lower
Drakensberg Group	Intercalated in Karoo basalts	Southern Namibia	Jurassic, Lower
Kalkrand Fm.	Karoo flood basalt province	Namibia	Jurassic, Lower
Mercia Mudstone Group	North Atlantic rift basins	Southern Britain	Triassic, Upper
Passaic and Lockatong Fms.	Newark Basin	Eastern North America	Triassic, Upper
Blomiden redbeds	Fundy Basin	Nova Scotia	Triassic, Upper
Buntsandstein	Helgoland Basin	East Greenland	Triassic, Middle
Pingdiquan Fm.	Junggar Basin	NW China	Permian, Upper
Groden Fm.	Intermontane basins, Alps	Tyrol, Austria	Permian, Upper
Opeche Shale	Williston Basin	North Dakota, USA	Permian, Middle
Nippewalla Group	Continental interior sag basins	Kansas, USA	Permian, Middle
Rotliegende sediments	Muhlhausen and Ilfeld basins	Germany	Late Carboniferous-Permian
Old Red Sandstone (middle)	Orcadian Basin	Scotland	Devonian, Lower
Parakeelya Alkali Member	Officer Basin	Australia	Cambrian

Table 3. Selected pre-Quaternary lacustrine evaporite examples classified by age and tectonic setting (see Warren 2016; Chapter 5 for deposit details and listing of relevant citations)

ancient lacustrine salts accumulated in endorheic or highly restricted discharge basins, with perennial saline water masses tending to occur in the drainage sumps of steep-sided drainage basins (Warren, 2010, 2016). Saline lake basins accumulating gypsum, or more saline salts like halite or glauberite, typically have a shallow water table in peripheral saline mudflat areas and so are dominated by continental sabkha textures. Nearby is the lowermost part of the lacustrine depression or sump where deposition is typified by ephemeral ponded brine pan deposits, rather than permanent saline waters.

Saline lacustrine mineralogies depend on compositions of inflowing waters, so depositional sumps in regions with non-marine ionic proportions in the feeder inflow, accumulate thick sequences of nonmarine bedded salts dominated by trona, glauberite, and thenardite. In contrast, nonmarine areas with thalassic (seawater-like) inflows tend to accumulate more typical sequences of halite, gypsum, and anhydrite.

Across the Pliocene-Quaternary icehouse, less-saline perennial saline-lake beds tend to occur during more humid climate periods in the same continental-lacustrine depressions where saline-pan beds form (e.g., Lake Magadi, Great Salt Lake, Lake Urmia). On a smaller scale, in some modern saline lake basins, parts of the lake floor can be permanently located below the water surface (Northern Basin in the Dead Sea or Lake Asal). In some modern saline sumps dominated by mudflats, a perennial saline lake water mass is located toward the edge of a more central salt-flat zone, forming a perennial water filled "moat" facies surrounding a seasonally desiccated saline pan (as in Salar, de Atacama, Salar de Uyuni, Lake Magadi, Lake Natron). These permanent to near-permanent saline water "moat" regions are typically created where fresher inflows encounter saltier beds of the lake centre, dissolve them, and so form water-filled peripheral depressions.

Bottom sediment in the moats tends to be mesohaline carbonate laminites, which can contain TOC levels as high as 12%.

High-water stage perennial saline lacustrine sediments tend to be carbonate-rich or silica-rich (diatomaceous) laminites. Ancient examples of large saline lacustrine deposits made up of alternating humid and desiccated lacustrine units include the Eocene Green River Formation of Wyoming and the Permian Pingdiquan Formation of the Junggar Basin, China (Table 4). Evaporites deposited in a suprasealevel lacustrine basin (especially Neogene deposits) have numerous same-scale Quaternary analogues, unlike the more voluminous ancient marine platform and basinwide evaporites (Figure 7). Clearly, across the Quaternary, saline continent lacustrine settings possess areas of bedded salt accumulation that are far greater than those of any contemporaneous marine-fed salt sumps. But in ancient climes, especially during in the continental interior of the Pangean supercontinent (mid Permian to Triassic), regions of continental interior sabkhas and saline pans had areas far greater than any seen in Quaternary continental saline sumps (Zambia and Benison, 2013).

Is the present-day climate the key to evaporite understanding?

This short answer is yes, Hadley Cells across the Phanerozoic are mostly tied to climate belts that maintain sub-tropical positions, but to this notion, we must add a geological context. Today we are living in an icehouse climate mode and have been for the last 12 Ma. It is tied to the presence of polar ice-sheets that wax and wane over 100,000-year time frames, so moving the position of the Hadley cells and changing the intensity of atmospheric circulation. In this icehouse climate, large eustatically-controlled marine-fed evaporite deposits are not preserved,

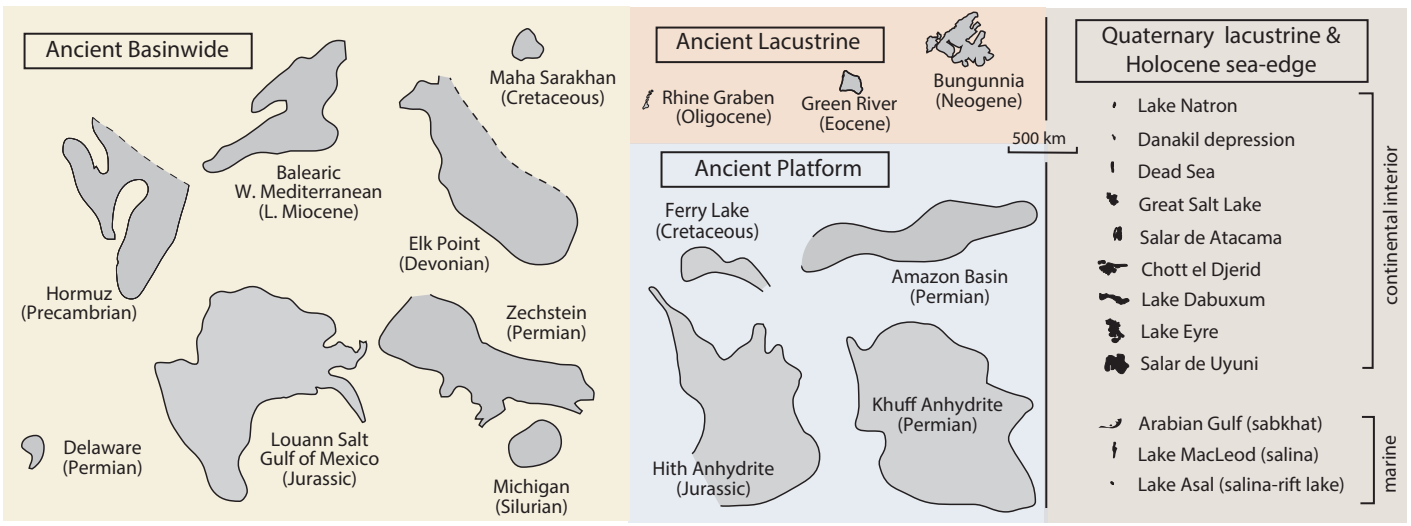

Figure 7. Comparison in depositional extent of modern and ancient evaporites (after Warren, 2016)

as sea level falls off the continental shelf every 100,000 years or so. The world's largest bedded salt deposits formed sometime in the last 2 million years, are found in continental interiors, typically in endorheic tectonic sumps in either hot arid or steppe climate settings, often with salt diapirs outcropping or subcropping in the drainage basin and the basin floor can be located at elevations well above sealevel (Part 1; Salty Matters, Tuesday, January 31, 2017).

As we move back into much of Phanerozoic time, we see world climates dominated by greenhouse modes, with shorter episodes of polar ice-sheets and icehouse climates in the Carboniferous-Early Permian ≈ 50 million years long, and the Ordovician, some 15 million years long (Figure 1). Greenhouse climate lacks permanent polar ice sheets, so sea-levels are higher, and 4th-order eustatic amplitudes in sea level are much less (a few meters versus hundred meters plus changes). Greenhouse sets up epeiric and intercontinental seaways that when hydrographically isolated, but still marine-fed, can deposit huge areas of platform evaporites centred in isolated seepage-fed sub-sealevel sumps. These platform deposits can also form outside of Greenhouse times in marine-fed tectonically-induced intracratonic sumps.

Basinwide evaporite deposits span icehouse and greenhouse mode arid belts, whenever a marine-fed subsealevel tectonic sump forms at positions of continent-continental proximity in an arid belt. Across much of the Phanerozoic, basinwide deposits typically accumulated beneath subtropical belts of cool, dry descending air set up in a Hadley cell, and so are located north and south of a tropical equatorial belt. But the accretion of the Pangaean supercontinent (Carboniferous to Jurassic) set up conditions of continentality and orographic shadowing that allowed an arid saline belt to span the hyperarid interior of the supercontinent.

References

Boucot, A., Chen-Xu, and C. Scotese, 2013, Phanerozoic Paleoclimate: An Atlas of Lithologic Indicators of Climate: Concepts in Sedimentology and Paleontology, v. 11: Tulsa, OK, SEPM, 32 p.

Chen-Xu, A. J. Boucot, C. R. Scotese, F. Junxuan, W. Yuan, and Z. Xiujuan, 2012, Pangaean aggregation and disaggregation with evidence from global climate belts: Journal of Palaeogeography, v. 1, p. 5-13.

Crowley, T. J., and G. R. North, 1991, Paleoclimatology: New York, Oxford University Press, 339 p.

Hudec, M. R., and M. P. A. Jackson, 2007, Terra infirma: Understanding salt tectonics: Earth-Science Reviews, v. 82, p. 1-28.

Lu, J., G. A. Vecchi, and T. Reichler, 2007, Expansion of the Hadley cell under global warming: Geophysical Research Letters, v. 34.

Parrish, J. T., 1993, Climate of the Supercontinent Pangea: Journal of Geology, v. 10.

Ruch, J., J. K. Warren, F. Risacher, T. R. Walter, and R. Lanari, 2012, Salt lake deformation detected from space: Earth and Planetary Science Letters, v. 331-332, p. 120-127.

Sweet, A. C., G. S. Soreghan, D. E. Sweet, M. J. Soreghan, and A. S. Madden, 2013, Permian dust in Oklahoma: Source and origin for Middle Permian (Flowerpot-Blaine) redbeds in Western Tropical Pangaea: Sedimentary Geology, v. 284,Äì285, p. 181-196.

Warren, J. K., 2010, Evaporites through time: Tectonic, climatic and eustatic controls in marine and nonmarine deposits: Earth-Science Reviews, v. 98, p. 217-268.

Warren, J. K., 2016, Evaporites: A compendium (ISBN 978-3-319-13511-3): Berlin, Springer, 1854 p.

Zambito, J. J., and K. C. Benison, 2013, Extremely high temperatures and paleoclimate trends recorded in Permian ephemeral lake halite: Geology, v. 41, p. 587-590.

Ziegler, A. M., S. F. Barrett, C. R. Scotese, and B. W. Sellwood, 1981, Palaeoclimate, Sedimentation and Continental Accretion [and Discussion]: Philosophical Transactions of the Royal Society of London. Series A, Mathematical and Physical Sciences, v. 301, p. 253-264.

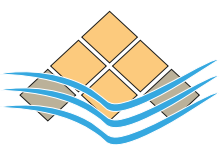

John Warren, Chief Technical Director
SaltWork Consultants Pte Ltd (ACN 068 889 127)
Kingston Park, Adelaide, South Australia 5049

www.saltworkconsultants.com